Initial growth of Mg films on Ru(0001): An efficient approximation scheme for the LEED analysis of incommensurate structures

S. Schwegmann, H. Over,* M. Gierer, and G. Ertl
Fritz-Haber-Institut der Max-Planck-Gesellschaft, Faradayweg 4-6, D-14195 Berlin, Germany
(Received 27 November 1995)

The epitaxial growth of incommensurate Mg layers on a Ru(0001) surface is investigated in the coverage range from submonolayers to 3 ML by analyzing low-energy electron-diffraction LEED $I(V)$ data. For the analysis of the 2-ML Mg film, we developed an efficient approximation scheme that allows the determination of mean interlayer spacings without employing the full unit cell. The Mg-Ru spacing is found to be 2.32 ± 0.05 Å, regardless of the presence of further Mg layers above. The Mg-Mg layer spacing in the Mg bilayer is 5%, expanded with respect to the value of the bulk material, while this layer spacing is expanded by only 2.5% after completion of the third Mg layer. The *ABAB*... stacking sequence is established from the beginning of the film growth.

I. INTRODUCTION

The growth of metal films on metal substrates has frequently been observed to proceed in a pseudomorphic way; i.e., below a critical thickness the overlayer is constrained to match the substrate lattice,[1] which usually induces strain fields in the metal film. If, however, the lateral interaction between the adsorbed metal particles is strong and dominates over the corrugation potential imposed by the underlying substrate, the growth of metal films takes place in an incommensurate manner; i.e., the metal film has its own periodicity which may not be related to substrate periodicity. As a result, these films are almost unstrained. The incommensurate structures are commonly modeled by relatively large unit cells in which the adatoms occupy inequivalent adsorption sites, while the atoms in these layers are evenly spaced.

A prototypical example for such a system represents the growth of Mg films on Ru(0001),[2] for which a succession of incommensurate superstructures was shown to exist in the submonolayer and multilayer-coverage region. In the submonolayer range, Mg forms islands which coalesce with increasing coverage until a uniform and homogeneous Mg overlayer is generated. The unit cell of this overlayer can be approximated by a (5×5) cell which leads to dominating $(h\frac{4}{5},k\frac{4}{5})$ (h and k integers) and weak multiple-scattering spots in low-energy electron diffraction (LEED). This kind of LEED pattern is characteristic of incommensurate structures. For the case of the (5×5) cell, 16 homogeneously distributed Mg atoms in the unit cell are adsorbed in different sites over 25 Ru atoms, so that the overlayer represents a $(\frac{5}{4}\times\frac{5}{4})$ structure to a first approximation.

Further uptake of Mg is then not used to build a second layer, but is instead incorporated into the first layer as evidenced by the corresponding LEED patterns: The (5×5) overlayer compresses continuously into a (7×7) structure with 36 Mg atoms per 49 Ru atoms, which corresponds to saturation of the monolayer with an absolute coverage of $\theta=0.75\pm0.03$ as judged from thermal-desorption spectra. The interatomic Mg distance agrees with that known for bulk Mg. Further Mg deposition then leads to the formation of the second layer, which is followed by the third layer after its completion, and so forth. Thus this (7×7) layer can be viewed as the nucleation plane for the subsequent layer-by-layer growth.

In a previous study,[2] LEED $I(V)$ data for only the 9-ML-thick Mg film were taken and analyzed. However, in order to understand and elucidate the initial steps of the Mg growth on Ru(0001), here we present additional LEED $I(V)$ data for the submonolayer regime along with those of ultrathin Mg films up to 4 ML. The ultrathin multilayer Mg films were analyzed by employing an efficient approximation scheme.

II. EXPERIMENT AND CALCULATIONS

The experiments were conducted in an ultrahigh-vacuum chamber (base pressure 1.2×10^{-10} mbar). The LEED facility consists of a four-grid optics. The LEED $I(V)$ curves were acquired from the fluorescence screen using a computer-controlled video-LEED system.[3] Magnesium was evaporated from a well-outgassed home-made source consisting of a small piece of Mg wire (purity 99.5%) wrapped in Ta foil, which was resistively heated. The typical deposition rate of Mg was about 0.5 ML/min at a sample temperature of 300 K. The relative Mg coverage was determined by integrating thermodeposition spectra (TD spectra) from which the absolute coverage was determined by assuming a coverage of 0.75 at the completion of the compression phase.[2] Varying Mg coverages in the submonolayer regime up to 2 ML were achieved by evaporating Mg multilayers and subsequently heating to specific temperatures in order to desorb excess Mg; note that the first and second Mg layer can readily be distinguished in TD spectra.[2] Mg films with more than two layers were prepared directly by depositing a certain amount of Mg at room temperature, since in the multilayer range (>2 ML) Mg from the third and the following layers comes off the surface at about the same temperature. For LEED $I(V)$ measurements, the sample was always cooled to 50 K. Further details about the experimental setup can be found in Refs. 4 and 5.

Fully dynamical LEED calculations were performed with the program package of Moritz.[6] Nine relativistically calculated phase shifts for Mg and Ru were used; details about the

 © 1996 The American Physical Society

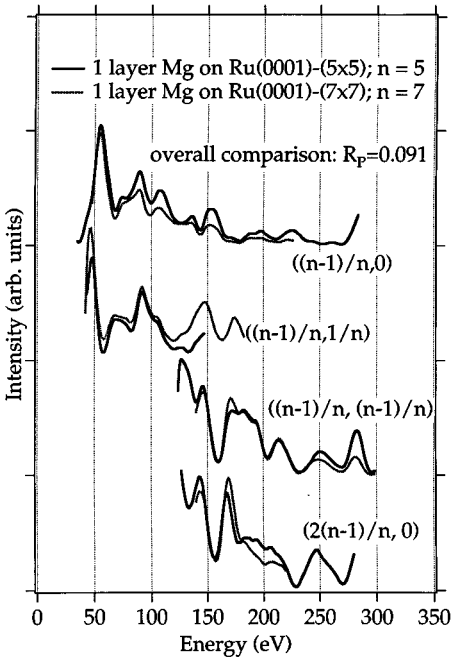

FIG. 1. Experimental LEED $I(V)$ curves at the beginning and the completion of the compression phase. The striking similarity indicates that the main structural elements in both overlayers are the same. For the Mg film throughout the submonolayer regime, a (5×5) unit cell can be used for LEED simulations.

computation of the phase shifts can be found elsewhere.[2,4] The agreement between calculated and measured $I(V)$ curves was quantified by using Pendry's r factor R_P.[7] The submonolayer Mg film on Ru(0001) was analyzed by applying an automated search method based on a nonlinear least-squares optimization scheme.[8] The functional to be minimized could be chosen alternatively: The least-squares sum either of intensities or of Y functions, according to the reliability factors R_{DE} as introduced by Kleinle *et al.*[9] and the Pendry R_P,[7] respectively.

III. RESULTS AND DISCUSSION

A. Submonolayer regime

In Fig. 1, the experimental $I(V)$ curves of the dominant Mg LEED spots up to the fourth order of the incommensurate (5×5) structure are compared with corresponding beams of the (7×7) structure which appeared after completion of the compression phase. Both sets of $I(V)$ data are strikingly similar, as also indicated by the corresponding overall R_P factor of 0.09, so that a (5×5) unit cell can be used for LEED simulations throughout the submonolayer regime, thus saving computing time. This striking similarity tells us that the $I(V)$ curves of the dominant Mg-induced LEED spots contain only very limited information about the adsorption sites of individual Mg atoms, since during the compression phase the adsorption sites of Mg change while the LEED $I(V)$ curves do not. The main information these beams carry are therefore the adsorbate-substrate-interlayer spacings, i.e., the structural parameters projected onto the $(\frac{5}{4}\times\frac{5}{4})$ or $(\frac{7}{6}\times\frac{7}{6})$ unit cell, which are similar in both cases. The insensitivity of LEED $I(V)$ curves to the adsorption site

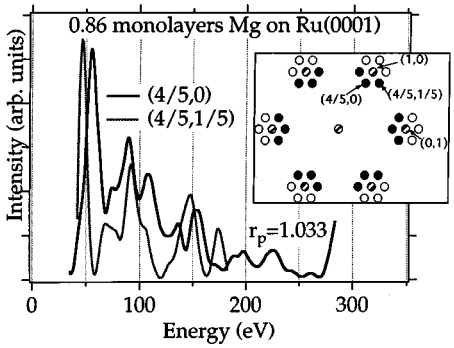

FIG. 2. Experimental LEED $I(V)$ curves of the $(\frac{4}{5},0)$ and $(\frac{4}{5},\frac{1}{5})$ beam. Although these beams are close in k space, the $I(V)$ curves are very different due to the involvement of different scattering paths and the sensitivity to different structural elements. While the $(\frac{4}{5},0)$ beam is sensitive to the averaged geometry with $(\frac{5}{4}\times\frac{5}{4})$ symmetry, i.e., the Mg-Ru layer spacing, the $(\frac{4}{5},\frac{1}{5})$ is affected strongly by the deviations from the $(\frac{5}{4}\times\frac{5}{4})$ symmetry.

in incommensurate overlayers is plausible because the adsorbate resides in various adsorption sites, and the scattering matrix of the adsorbate layer represents a sum over the Mg atoms (modified by a geometrical phase factor) which corresponds to a kind of averaging over different Mg adgeometries. The insensitivity of the LEED $I(V)$ curves to varying intraplane Mg-Mg distances is due to weak intralayer scattering. A similar effect has recently been observed for the system Li on Ru(0001), where the incommensurate (5×5) structure containing 16 Li atoms could be well approximated by a (5×1) unit cell containing only four Li atoms.[10] In addition, the dominant $[h(n-1)/n,\ k(n-1)/n]$ LEED spots [h and k integers, $n=5$ for the (5×5) and $n=7$ for (7×7) structure] are close in **k** space and—as long as the scattering paths are similar—the $I(V)$ curves are similar. However, we want to point out that the mere proximity of beams in **k** space is not sufficient for the similarity of LEED $I(V)$ curves, as demonstrated in Fig. 2. This figure shows $I(V)$ curves of the $(\frac{4}{5},0)$ and the $(\frac{4}{5},\frac{1}{5})$ beam. Although these beams are close to each other in **k** space, the $I(V)$ curves differ substantially ($R_P=1.03$), consistent with different dominating scattering paths being involved: the $(\frac{4}{5},0)$ beam contains single scattering events, while the $(\frac{4}{5},\frac{1}{5})$ does not.

We turn now to the LEED structure analysis of the (5×5) Mg overlayer. The analysis was based on a data set which consists of five fractional and two integer-order beams in an energy range of 50–280 eV, resulting in a cumulative energy range of 1220 eV. In line with the above discussion, the structure analysis of Mg (5×5) was most sensitive to the Mg-Ru layer spacing, which turned out to be 2.33 ± 0.04 Å. Lateral displacements of the Mg atoms toward threefold hollow-site positions by up to 0.3 Å (cf. Fig. 3) could further improve the agreement between experimental and calculated LEED $I(V)$ curves. The improvement mainly concerns the $(\frac{4}{5},\frac{1}{5})$ beam, a true multiple-scattering spot which is heavily affected by deviations of the overlayer geometry from the $(\frac{5}{4}\times\frac{5}{4})$ periodicity. The same improvement in the R factor could be achieved by introducing a buckling of about 0.15 Å in the Mg layer. In fact, it turned out to be impossible to favor one of these two possibilities on the basis of the present data set. Presumably, more multiple-scattering spots

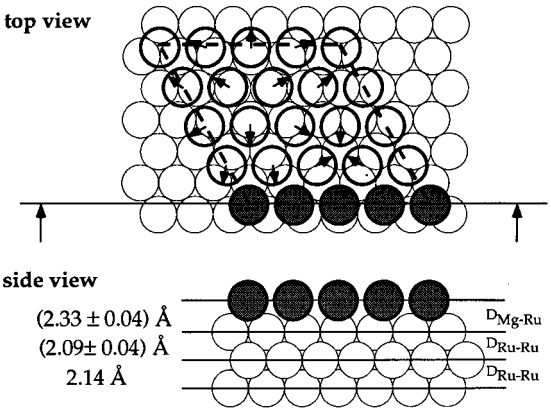

FIG. 3. Structural parameters of the submonolayer Mg film on Ru(0001). The arrows in the top view indicate the direction of possible lateral displacements as suggested by the LEED analysis. The main effect is that Mg atoms sitting near the on-top position are drawn toward hollow sites by up to 0.3 Å.

have to be included in the analysis to resolve this ambiguity. Since these spots are weak and close to bright spots, reliable measurements are not possible. However, as indicated by the intense $(\frac{4}{5},0)$ and related higher-order beams in the LEED pattern, the Mg arrangement in the submonolayer region consists of an almost evenly dispersed overlayer with only slight lateral and/or vertical distortions. The Mg-Ru layer spacing has to be considered as a mean layer spacing. The first Ru-Ru layer spacing with 2.09 ± 0.04 Å is equal to that found for the bare Ru(0001) surface. Figure 4 displays the experimental LEED $I(V)$ data compared to $I(V)$ curves calculated for the optimum Mg overlayer geometry; the overall Pendry r factor is 0.36.

B. Geometry of the two-monolayer Mg film

After compression of the first Mg monolayer, the (7×7) LEED pattern persists upon growth of further Mg

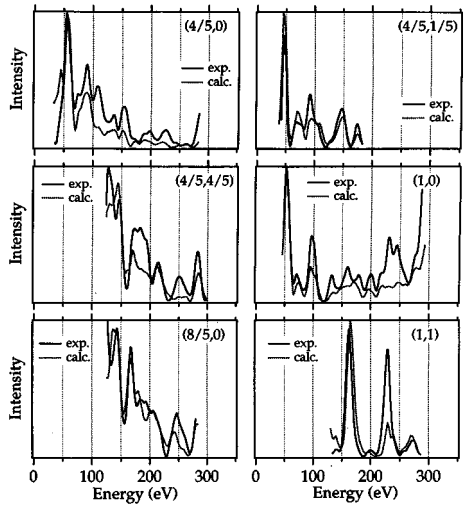

FIG. 4. Experimental and calculated LEED $I(V)$ curves for the best-fit geometry of a 0.85-ML-thick Mg film on Ru(0001) ($\theta_{Mg}=0.64$). The Pendry R factor is 0.36. The corresponding structural parameters are given in Fig. 3.

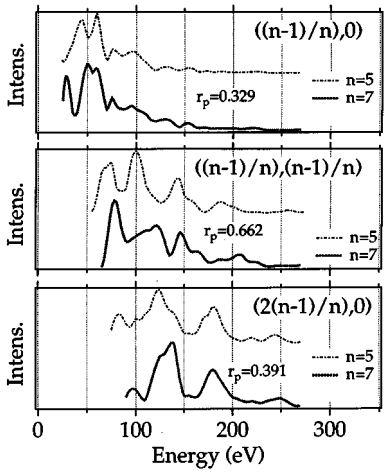

FIG. 5. Calculated LEED $I(V)$ curves using (5×5) and (7×7) symmetries for the bilayer Mg film on Ru(0001). The substantial difference in these curves, quantified by an averaged Pendry R factor of 0.39, demonstrates that for multilayer Mg films the actual unit cell, namely the (7×7), and not the (5×5) symmetry has to be chosen.

layers. Due to the second Mg layer, interlayer forward scattering between the ordered Mg planes becomes important, and hence it is not clear whether the approximation of a (5×5) unit cell is still appropriate for the simulation of the Mg bilayer. Indeed, the reduction of a (7×7) into a (5×5) unit cell is only a poor approximation, as can be judged from Fig. 5. This figure displays a comparison between calculated LEED $I(V)$ curves of dominant LEED beams for (5×5) and (7×7) structures having the same interlayer spacings. In the measurements only the dominant Mg beams were considered, since for more than 1-ML Mg the multiple-scattering spots are too weak and too close to bright LEED beams, so that proper background corrections turned out to be problematic.

Hence we are left with the problem of computing LEED $I(V)$ curves of a two-layer (7×7) structure, each layer containing 36 Mg atoms in the unit cell. The imposed symmetry $(p3m1)$ of the structure allows for a reduction of 36 atoms per layer in the unit cell to nine and ten nonequivalent atoms in the first and second Mg layers, respectively. However, the computational effort for the calculation of the LEED $I(V)$ curves is enormous. Since only the dominant Mg beams were measured, the main information we can expect to obtain from this analysis is the averaged geometry [the geometry projected onto the $(\frac{7}{6}\times\frac{7}{6})$ unit cell], i.e., the layer spacings. This whole situation calls for an efficient approximation scheme. In searching for such an approximation, we recognized that, due to the close proximity of the dominant (7×7) spots to the integer-order beams, a mixing between the dominant Mg and (1×1) substrate beams is small for all but the (0,0) beam because either scattering paths with large momentum transfer at the bulk interface are involved [cf. Fig. 6(a)], or interlayer scattering between bulk and overlayer with at least one backscattering event at the overlayer is required [cf. Fig. 6(b)]. Thus the nondiagonal elements of the bulk scattering matrix may be neglected for the computation of the $I(V)$ curves of dominant Mg beams. In addition (cf. Sec. III A), Mg occupies many different ad-

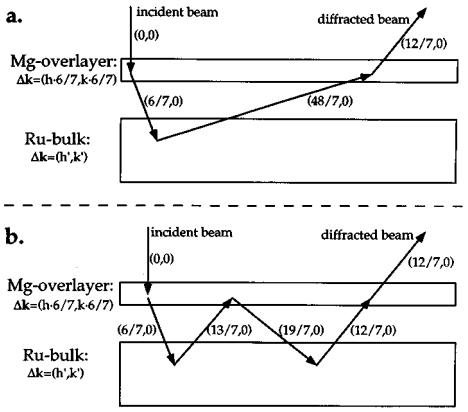

FIG. 6. Two types of multiple-scattering paths that cause intermixing of dominant Mg beams with those of (1×1) symmetry due to nondiagonal elements of the bulk scattering matrix. (a) This scattering event is negligible since a large momentum transfer imposed by the bulk is involved. (b) The scattering paths can be neglected because backscattering at the overlayer is required.

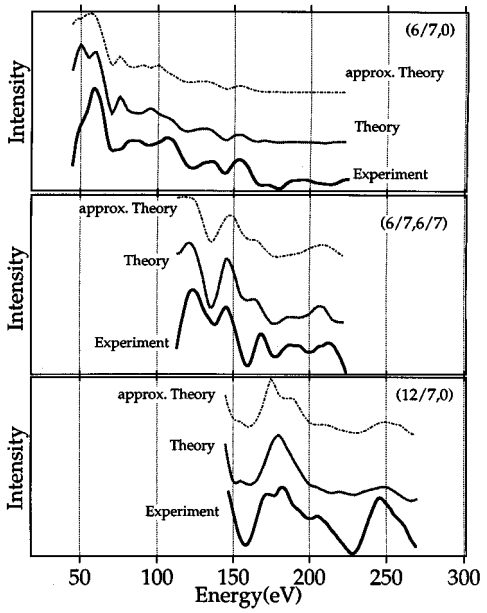

FIG. 7. Comparison of experimental LEED $I(V)$ curves with calculated LEED $I(V)$ curves using the full multiple-scattering scheme ($R_P=0.37$) and the mirror approximation ($R_P=0.42$). The optimum real-space model turned out to be the same for both cases, and is given in Fig. 8.

sorption sites, and therefore only the bulk reflection matrix averaged over these local registries participates in the scattering between the Mg film and the substrate. Again, this averaging causes only the diagonal elements of the reflection matrix to survive. Altogether, the substrate in the multiple-scattering process between the Mg film and the substrate acts more like a mirror than a template with atomic structure; i.e., all beams coming from the Mg film are backscattered in the specular direction.

With this knowledge in mind, we can try to erect the following approximation scheme: The evenly dispersed Mg overlayer is considered as a $(\frac{7}{6}\times\frac{7}{6})$ structure above the (1×1) substrate. The scattering properties of the substrate are taken into account by the diagonal elements of its reflection matrix only. This restriction of the bulk reflection matrix to diagonal elements corresponds to treating the bulk as an ideal mirror. Up to now, we could not save much computing time, since we still have to calculate the scattering amplitude of all beams associated with the (7×7) structure. However, we are only interested in those $I(V)$ curves which are associated with the $(\frac{7}{6}\times\frac{7}{6})$ unit mesh since only these beams were measured. We therefore introduce the following crucial approximation: In angular momentum space, the scattering matrices of each bulk plane is calculated for the (1×1) geometry (especially the lattice sum), and is then projected only into those directions (LEED beams in **k** space) which are associated with the $(\frac{7}{6}\times\frac{7}{6})$ unit cell. Only the diagonal elements of the reflection matrices are then used, and the multiple scattering between the bulk planes is not considered, so that each of the bulk planes serves as a mirror for beams coming from the Mg overlayers. Altogether, LEED $I(V)$ calculations are now performed with a modified (1×1) Mg overlayer over a substrate acting solely as an ideal mirror with a density of Ru atoms which corresponds to Ru bulk; this approach will be called the *mirror approximation*. The computational effort for this approximation is the same as for the calculations of a (1×1) structure, and hence tremendously reduced if compared with the full (7×7) unit cell; typically the computing time could be reduced by a factor of 30.

A comparison of experimental LEED $I(V)$ curves with those calculated for the optimum Mg geometry using full multiple scattering and the approximations outlined above is displayed in Fig. 7. The corresponding Pendry r factors between experiment and theory do not change very much (from 0.37 to 0.42) when applying full and restricted multiple scattering to the same Mg-film geometry, respectively. The optimum geometry of the 2-ML Mg film on Ru(0001) is indicated in Fig. 8, and has the following characteristics: The Mg-Ru interlayer spacing (2.32 ± 0.05 Å) is not affected by the presence of the second Mg layer if compared with a single Mg overlayer on Ru(0001) (cf. Sec. III A). The

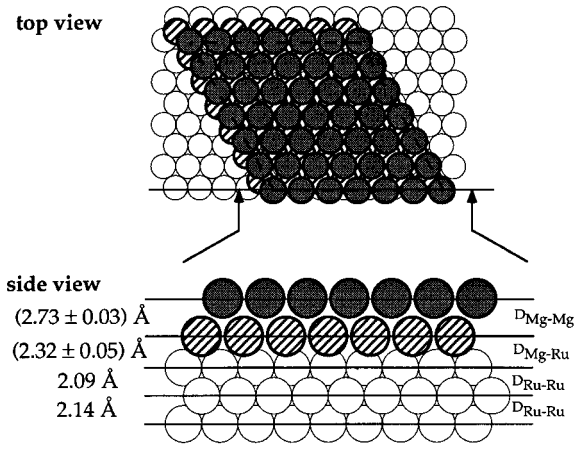

FIG. 8. The optimum structure parameters derived for the 2-ML-thick Mg film on Ru(0001).

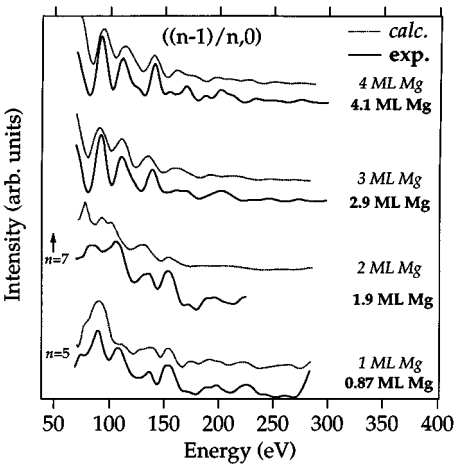

FIG. 9. Evolution of the experimental LEED $I(V)$ curves of the lowest-order Mg beam with the Mg coverage in comparison with corresponding curves calculated for the optimum geometry of that Mg film (''mirror approximation'' applied for $\geqslant 2$ ML). The saturation behavior compares well, which is strongly indicative of the layer-by-layer-growth of Mg on Ru(0001) without any stacking fault.

Mg-Mg layer spacing turned out to be $(2.73 \pm 0.03$ Å), which is expanded by 5% with respect to the Mg(0001) bulk layer spacing (2.60 Å). This value is even expanded if compared to the topmost layer spacing found for the 9-ML Mg film and Mg(0001) $(2.64 \pm 0.04$ Å).[2,11] The expansion of the outermost Mg-Mg layer spacing with respect to the bulk value has been traced back to the s-p hybridization necessary to form a bonding between Mg atoms;[12] note that the valence shell of Mg $(3s^2)$ is full. This hybridization costs a substantial amount of energy (about 2.7 eV) which is compensated for by the energy gain due to the improved bonding between Mg atoms. On the surface this gain is smaller, since the Mg atoms in the outermost layer are less coordinated than Mg in the bulk. The total energy of the surface can therefore be minimized by reducing the hybridization, which, in turn, causes the observed expansion of the Mg-Mg layer spacing. Within the given limits of precision, the structural results of the 2-ML Mg film are the same when using full multiple-scattering theory or applying the mirror approximation, thus giving confidence to the mirror approximation.

One can anticipate that the mirror approximation will work even more accurately for heavier adsorbate atoms than Mg, since the diffraction intensity is then dominated by the overlayer. Therefore, we anticipate a wide application of the mirror approximation in the structure analysis of incommensurate metal films on metal substrates. A more rigorous treatment of incommensurate structures (considered as modulated structures) has been developed very recently by Grünberg and Moritz.[13] This method not only allows one to solve the averaged geometry of an incommensurate metal film, i.e., the mean layer spacings, but is also able to determine periodic modulations. However, the computational effort is considerable.

C. Morphology of multilayer Mg films on Ru(0001)

To investigate the mode of Mg-film growth on Ru(0001), Fig. 9 (full lines) shows the evolution of the $[(n-1)/n,0]$ beam with progressing Mg deposition [$n=5$ and 7, depending on whether the (5×5) or the (7×7) structure is considered]. Obviously, the main features in the $I(V)$ data have already been developed with about 3-ML Mg; the coverage is based on the integral of the corresponding TD spectrum. Further increase of the Mg coverage results only in a fine structuring of the $I(V)$ curves at higher electron energies ($\geqslant 200$ eV) and eventually saturates at about 4 ML; compare the $I(V)$ curve for 2.9 ML with that of 4.1 ML. Figure 9 (dotted lines) displays the evolution of calculated LEED $I(V)$ curves (always calculated for the optimum geometry of that Mg film) of the first Mg-induced beam with coverage; for the submonolayer regime a (5×5) unit cell was used, and for more than one ML the mirror approximation was applied. Also with the calculated LEED $I(V)$ curves, the main features are developed at about 3 ML, and saturation takes place at about 4-ML Mg if the regular $(ABAB\ldots)$ stacking sequence of Mg(0001) is used. This comparison strongly supports that the growth of Mg on Ru(0001) proceeds in a layer-by-layer fashion. In addition, the optimization of the interlayer spacings for the 3- and 4-ML film shows that the pronounced expansion of the topmost Mg-Mg layer spacing for the bilayer film is reduced to 2.68 ± 0.04 Å, which compares well to the value for the Mg bulk [2.64 Å (Ref. 11)].

IV. CONCLUDING REMARKS

In this paper we investigated the initial growth of Mg on Ru(0001) on the basis of the analyses of LEED $I(V)$ curves and its evolution with Mg deposition. In the submonolayer regime, Mg forms islands of incommensurate structures which can be described as a (5×5) containing 16 Mg atoms. These islands coalesce into a homogeneous (5×5)-16 Mg overlayer. Further uptake of Mg then leads to a compression of this layer from a (5×5)-16 Mg into a (7×7)-36 Mg structure which serves as a nucleation plane for the subsequent layer-by-layer growth with (7×7) symmetry. The $I(V)$ curves of the dominant LEED beams associated with a $(\frac{5}{4}\times\frac{5}{4})$ or $(\frac{7}{6}\times\frac{7}{6})$ unit cell are very similar up to the completion of the first Mg monolayer, although the Mg atoms have to change their local adsorption sites during the compression phase. This similarity can be interpreted as experimental evidenced that no information on the adsorption site of individual atoms in an incommensurate overlayer is accessible as long as only the dominant single-scattering beams are analyzed. The only parameter which can be extracted is the mean Mg-Ru interlayer spacing: 2.33 ± 0.04 Å. The (5×5) symmetry can be used in the analysis of the Mg overlayer throughout the compression phase. A hint on lateral distortions in the overlayer, i.e., the Mg atoms near the on-top position are shifted by $\leqslant 0.3$ Å toward the hollow sites, is supplied mainly by the $I(V)$ curve of the multiple-scattering $(\frac{4}{5},\frac{1}{5})$ beam.

For the analysis of Mg films with more than 1 ML, the scattering between the Mg atoms has to be modeled correctly, i.e., the use of the (5×5) symmetry is too crude an approximation. To avoid calculations with large unit cells [in our case (7×7)], we introduced the concept of the *mirror approximation*. This means that the Mg overlayer is treated as a $(\frac{7}{6}\times\frac{7}{6})$ structure, and for the multiple scattering between

Mg and Ru only the diagonal elements for the Ru bulk-scattering matrix are considered. Thus the Ru bulk serves as an ideal mirror for beams coming from the Mg overlayer. In order to have the proper Ru density in the bulk of Ru(0001), the scattering matrices in angular momentum space are calculated with the regular Ru(0001)-(1×1) structure, while the **k**-space projection is performed only in directions defined by the $(\frac{7}{6}\times\frac{7}{6})$ Mg overlayer. It is shown that the $I(V)$ data obtained by this approximation compares well with those obtained by full-dynamical calculations and, more importantly, the structural parameters turned out to be the same for both cases. The Mg-Ru layer spacing is 2.32 ± 0.05 Å and is therefore not affected by the presence of the second Mg layer. The Mg-Mg layer spacing is 2.73 ± 0.05 Å, which is expanded by 5% in comparison with the Mg(0001) bulk value (2.60 Å),[2] and even expanded with respect to the topmost layer spacing of Mg(0001) (2.64 ± 0.04 Å).[11]. With the completion of the third Mg layer, this excessive expansion is retracted.

As demonstrated by the evolution of the LEED $I(V)$ curves with Mg coverage in comparison with LEED simulations, the growth of Mg takes place in the expected $ABAB\ldots$ stacking sequence right from the beginning, and proceeds in a layer-by-layer fashion.

*Author to whom correspondence should be addressed.
Fax: ++49-30-84135106.
Electronic address: over@thi-berlin.mpg.de

[1] F. Jona and P. M. Marcus, in *Surface Physics and Related Topics*, edited by F. J. Yang, G. J. Ni, X. Wang, K. M. Zhang, and D. Lu (World Scientific, Singapore, 1990), p. 213, and references therein.

[2] H. Over, T. Hertel, H. Bludau, S. Pflanz, and G. Ertl, Phys. Rev. B **48**, 5572 (1993), and references therein.

[3] P. Heilmann, E. Lang, K. Heinz, and K. Müller, Appl. Phys. **9**, 247 (1976); K. Müller, E. Lang, L. Hammer, W. Grimm, P. Heilmann, and K. Heinz, in *Determination of Surface Structure by LEED*, edited by P. M. Marcus and F. Jona (Plenum, New York, 1984); K. Heinz, Prog. Surf. Sci. **27**, 239 (1988); D. von Gemünden, Ph.D. thesis, Universität Erlangen-Nürnberg, 1990.

[4] H. Over, H. Bludau, M. Skottke-Klein, G. Ertl, W. Mortiz, and C. T. Campbell, Phys. Rev. B **45**, 8638 (1992).

[5] H. Bludau, Ph.D. thesis, Freie Universität Berlin, 1992.

[6] W. Moritz, J. Phys. C **17**, 353 (1983).

[7] J. B. Pendry, J. Phys. C **13**, 937 (1980).

[8] G. Kleinle, W. Moritz, and G. Ertl, Surf. Sci. **238**, 119 (1990); H. Over, U. Ketterl, W. Moritz, and G. Ertl, Phys. Rev. B **46**, 15 438 (1992); M. Gierer, H. Over, and W. Moritz (unpublished).

[9] G. Kleinle, W. Moritz, D. L. Adams, and G. Ertl, Surf. Sci. **219**, L637 (1989).

[10] M. Gierer, H. Over, H. Bludau, and G. Ertl, Phys. Rev. B **52**, 2927 (1995).

[11] P. T. Sprunger, K. Pohl, H. L. Davis, and E. W. Plummer, Surf. Sci. **297**, 48 (1994).

[12] A. F. Wright, P. J. Feibelman, and S. R. Atlas, Surf. Sci. **302**, 215 (1994).

[13] T. Grünberg and W. Moritz (unpublished).